

ZrB₂-TiB₂ Nanocomposite Powder Prepared by Mechanical Alloying

Luo Ping^{1,2}, Dong Shijie^{1,2}, Yangli Anzhao², Sun Shixuan³, Xie Zhixiong², Zheng Zhong², Yang Wei²

¹ Huazhong University of Science and Technology, Wuhan 430074, China; ² Hubei Provincial Key Laboratory of Green Materials for Light Industry, Hubei University of Technology, Wuhan 430068, China; ³ Capital Aerospace Machinery Corporation, Beijing 100076, China

Abstract: Diborides, including zirconium diboride (ZrB₂) and titanium diboride (TiB₂), have a number of desirable ceramic qualities that make suitable for preparing ceramic-matrix composites. However, synthesizing a composite based on these materials usually requires high temperatures and complex synthetic methods. In the present study, a nanocrystalline ZrB₂-TiB₂ powder was synthesized via mechanical alloying (MA) of the mixture of elemental Zr, Ti, and B powders mixed at a Zr/Ti/B mole ratio of 1:1:4, a 10:1 ball-to-powder weight ratio and 500 r/min rotational speed in a planetary ball-mill under argon atmosphere using a ZrO₂ vial and balls. The effect of milling time on the phase change was investigated by X-ray diffraction (XRD), and the microstructure evolution of the powder mixture was monitored by field emission scanning electron microscopy (FESEM) and transmission electron microscopy (TEM). It is found that after 120 h of milling, a nanoscale composite powder with ~20 nm mean particle size can be obtained. Moreover, TEM examination clearly shows the composite powder is composed of the nanoscale TiB₂ and ZrB₂ particles. Finally, the milling mechanism was discussed.

Key words: ZrB₂-TiB₂; nanocomposite; mechanical alloying

Diborides from the transition metals IVB group, such as zirconium diboride (ZrB₂) and titanium diboride (TiB₂), exhibit high strength, excellent hardness, high melting point, high thermal and electrical conductivity, good thermal shock resistance and good chemically stability^[1-14]. Such a series of interesting properties make TiB₂ and ZrB₂ useful materials for commercial applications. Additionally, ceramic-matrix composites (CMCs) have gained increasing interest due to their enhancing intrinsically low fracture resistance of monolithic ceramics^[11-17]. The use of ZrB₂ and TiB₂ ceramics in composites is expected to offer a variety of high-temperature thermal and structural applications compared to individual ceramics. In order to improve mechanical properties, it is vital to prepare ZrB₂-TiB₂ powder with fine and homogeneous particles used as

composite precursors.

Since ZrB₂ and TiB₂ are covalent materials with low self-diffusion coefficients and high melting points, it is difficult to fabricate ZrB₂-TiB₂ composites using conventional sintering methods^[11-15, 17-19]. Currently, ZrB₂-TiB₂ composites are usually fabricated using a mechanical activation assisted self-propagating high-temperature synthesis of Zr/Ti/B powder blends^[11, 13, 15, 19], pressureless sintering^[18] or spark plasma sintering^[12, 15]. However, the methodology for producing fine structure ZrB₂-TiB₂ ceramic powders via mechanical alloying (MA) has not been covered in depth. MA is a solid-state powder processing technique involving repeated welding, fracturing, and re-welding of powder particles in a high-energy ball mill^[20, 21]. MA is superior to other methods due to its low

Received date: June 14, 2015

Foundation item: National Natural Science Foundation of China (51375150, 51205114); Academic Leaders Project of the Wuhan Science and Technology Bureau (201271130448); the Hubei Provincial Natural Science Foundation of China (2013CFB018)

Corresponding author: Dong Shijie, Ph. D., Professor, Hubei Provincial Key Laboratory of Green Materials for Light Industry, Hubei University of Technology, Wuhan 430068, P. R. China, Tel: 0086-27-59750777, E-mail: dongsj@163.com

Copyright © 2016, Northwest Institute for Nonferrous Metal Research. Published by Elsevier BV. All rights reserved.

cost, simplicity and high output. Several ceramic nanocomposites, including TiB₂-TiC nanocomposite powders^[22], nanocrystalline ZrB₂ powder^[18], and nanocrystalline Ti(C,N) powder^[23] others^[24] have been successfully fabricated using MA.

The present work described the preparation of ZrB₂-TiB₂ nanocomposites powders at ambient temperature using MA. The mole ratio of Zr:Ti:B used were 1/1/4. Effects of MA duration on the composition and the microstructure features of the composite powders was evaluated.

1 Experiment

Metallic zirconium powder (Zr, 99.5% purity, Sinopharm Chemical Reagent Co., Ltd, China), titanium powder (Ti, 99.99% purity, Sinopharm Chemical Reagent Co., Ltd, China), and amorphous boron powder (B, 99% purity, Sinopharm Chemical Reagent Co., Ltd, China) were used as the raw materials. They had irregular shapes and particle sizes between 1~50 μm (Fig.1a~1c).

The powders were mixed to obtain the mixture with a Zr/Ti/B mole ratio of 1:1:4. The MA experiments were carried out in a planetary ball mill (QM-3PS2, Nanjing

NanDa, China) using 8 mm diameter zirconia balls in a 250 mL zirconia vial with a ball-to-powder weight ratio (BPR) of 10:1. The powder mixture and the balls were placed inside the vials and sealed in a glove box (ZKX1, Nanjing NanDa, China) under Ar gas to prevent surface oxidation and contamination of the powder blends from the surrounding atmosphere. The formation of amorphous and nanocrystalline structures by MA is strongly dependent on the processing parameters. The most important processing parameters are the milling time, milling atmosphere, BPR and rotation speed. In the present work, we only changed the milling time while keeping the other parameters nominally constant: BPR at 10:1, rotation speed at 500 min⁻¹, and an argon shield. The MA process was interrupted at regular time intervals of 0, 10, 20, 40, 60, 80, 100, and 120 h, and a small portion of the powder was removed from the vial in the argon-filled glove box for characterization. Herein we defined the reaction initiation time when a sharp increase in the vial temperature was identified.

The phase evolution with milling time was investigated using an X-ray diffraction (XRD) analyzer (D8 Advance,

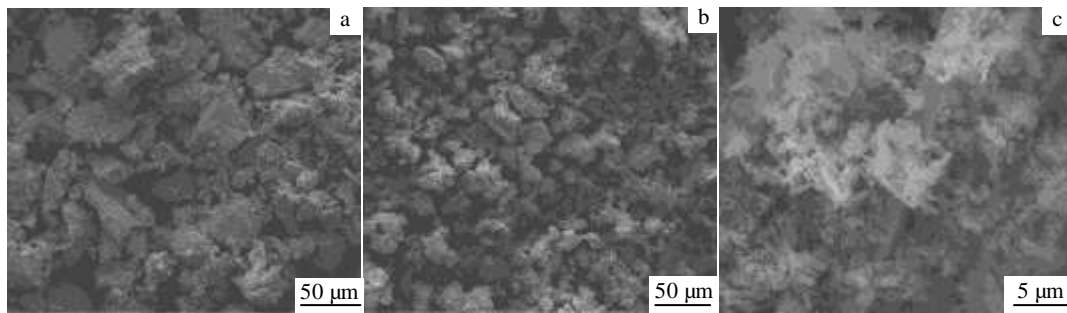


Fig.1 SEM morphologies of the starting powders: (a) Zr , (b) Ti, and (c) B

Bruker, Germany) with Cu Kα radiation. The scanning speed was 2°/min and two-theta was recorded across the range of 20° to 90° with a 0.02 step size. The morphologies of the powder mixtures after milling for different time intervals were observed via field-emission scanning electron microscopy (FESEM, NoVa Nano SEM 430, FEI Company, USA) and transmission electron microscopy (TEM, Tecnai G2 F20, FEI Company, USA).

2 Results and Discussion

2.1 XRD analysis of the powder mixtures

Fig.2 shows the XRD patterns for the mixtures of Zr, Ti, and B at a 1:1:4 mole ratio after MA for 0, 10, and 20 h. There is no boron peak due to its amorphous nature. It is evident in Fig.2 that no new phases are formed, the peak intensities decrease sharply after only short milling duration. The peak broadening in the XRD spectra results from increased internal strain and reduced grain size due to the

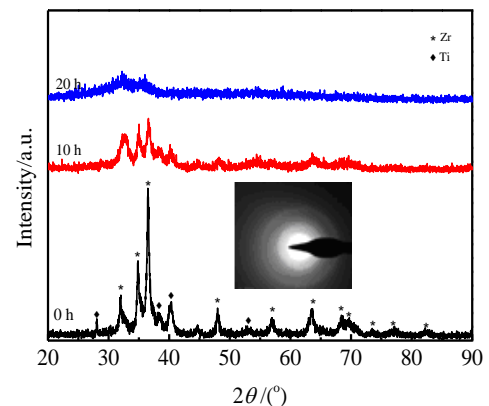


Fig.2 XRD patterns of the Zr/Ti/B powder blend at a mole ratio of 1:1:4, milled for different time (the inset shows the SAED pattern of the powder mixture milled for 20 h)

heavy deformation, repeated fracturing, and cold welding of the powder particles during MA (Fig.2b). As shown in Fig.2c, after 20 h continuous ball milling, all crystalline peaks disappear. Their disappearance means amorphous phase formation, which was confirmed by the selected area electron diffraction (SAED) pattern.

After 40 h of milling, strong XRD peaks for ZrB_2 and TiB_2 phases appear; however, no individual Zr or Ti peaks are observed, indicating reaction completion. These results illustrate that the ZrB_2 - TiB_2 reaction only requires a short time period to reach completion. Also, the higher and sharper XRD diffraction peaks of the reaction products (Fig.3a) may be attributed to the high temperature resulting from the release of high heat of formation. If further ball milling is carried out to 120 h, the characteristic XRD peaks are broadened and decreased in intensity, which may be attributed to a very fine grain size (see Fig.3b~3e).

2.2 Microstructure evolution

Fig.4a and 4b show the SEM images of the powder mixtures after milled for 10 h and 20 h, respectively, with the corresponding cross section micrographs shown as insets. Fig.4a illustrates that the initially ductile Zr and Ti particles are deformed into lamellar particles after the repeated cold welding and fracturing. A considerable quantity of B particles, appearing as black points in Fig.4a inset, are trapped between the flattened Zr and Ti particles during the early MA stage. Upon further milling this lamellar structure disappears (Fig.4b inset) and the uniformity of the B distribution is improved. A heavy plastic deformation can introduce more strain and a larger number of point defects are generated. An increased number of point defects can modify diffusion behavior as well as the crystalline structure chemical order, leading to an easier amorphization. This is confirmed via the powder mixture XRD analyses after 20 h of MA (Fig.2c), as well as their corresponding SAED pattern results. After 20 h of milling, an increase in the mean particle size can be observed as a result of the cold welding.

The morphology changes of the ZrB_2 - TiB_2 powder with increasing milling time are shown in Fig.5. At the early stages, the ZrB_2 - TiB_2 powder consists of coarse particles nearly spherical structures with an approximately 20 μm mean size after 20 h milling (Fig.4b and Fig.5a). With increasing of MA duration, the powder becomes more spherical, fine and homogenous (Fig.5b~5f). The fine grain structure of the particles can be explained by the hard ZrB_2 and TiB_2 phases acting as “micro-milling balls” during the MA process. These “micro-milling balls” compact, etch, cut mutually, and a friction is generated on the microscale, grains are further refined^[25].

Since it was difficult to clearly observe the fine structure of the powder by SEM, the TEM was employed. For the sake of simplicity, only the product obtained after 120 h of

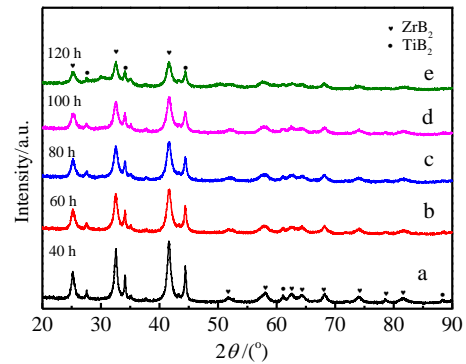


Fig.3 XRD patterns of the powder blended at a Zr/Ti/B mole ratio of 1:1:4, milled for different time

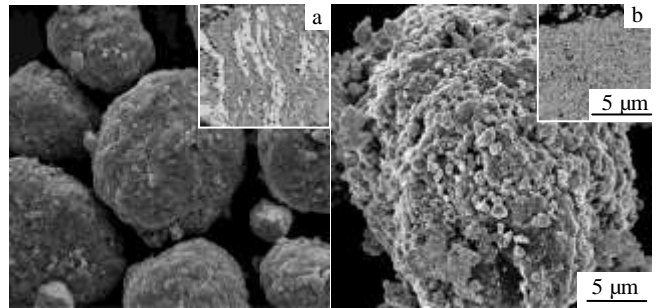


Fig.4 SEM morphologies of the powder milled for 10 h (a) and 20 h (b) (the insets show their corresponding cross section micrographs)

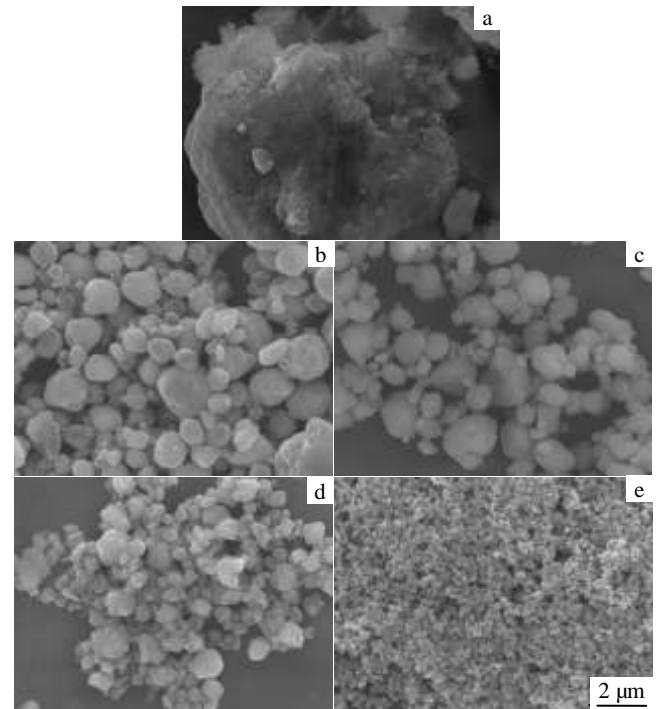


Fig.5 SEM images of the powder mixtures milled for different time: (a) 40 h, (b) 60 h, (c) 80 h, (d) 100 h, and (e) 120 h

milling was investigated by TEM and SAED patterns analyses (Fig.6). The SAED results reveal that the target products include monocrystalline ZrB_2 , TiB_2 particles (<20 nm in size, as shown in the insets of Fig.6a), and polycrystalline ZrB_2 - TiB_2 particles ~20 nm in size. The {001}, {100}, and {002} diffraction rings of ZrB_2 , and the {101} and {002} diffraction rings of TiB_2 are clearly observed in the SAED pattern as shown in Fig.6b. These findings further confirm that the powder mixture milled for 120 h consists of ZrB_2 and TiB_2 . Upon closer examination of the bright field image (Fig.6a), it is confirmed that the particles are formed by agglomeration. Additionally, nanoscale TiB_2 particles clearly form a composite with the ZrB_2 , resulting in the TiB_2 having a higher hardness than ZrB_2 ^[26,27].

2.3 Mechanisms of alloying

In our research, the ZrB_2 - TiB_2 nanopowder was synthesized by MA using Zr, Ti, and B as the starting materials. The alloying mechanism includes three stages. At the activation period (<20 h), Zr and Ti are soft and tend to weld together, forming a layered structure through the ball-powder-ball collisions. The brittle B particles are trapped between the Zr and Ti particles (Fig.4a inset) during this process. Upon further milling, the ductile powder particles are hardened with the lamellae becoming convoluted and refined. With continued milling, the lamellae become further refined with the brittle B particles which are uniformly dispersed in the Zr and Ti matrix (Fig.4b). These conditions promote the production of a variety of crystal defects, such as dislocations, vacancies, stacking faults, and the increase of number of grain boundaries. These defects increase the contact area between the components, supplying more diffusion channels which reduce the activation energy barrier.

After the powder mixture proceeds through the first reaction stage, it is subjected to an intense plastic deformation, and thoroughly mixed, refined, resulting in an increased number of structural defects. The frictional heat is generated during the ball mill process followed by the second stage (at 20 h to 40 h). Once the

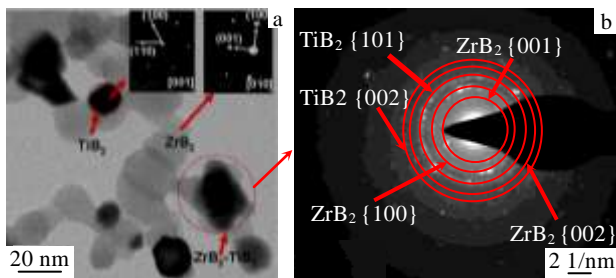


Fig.6 TEM images of an agglomerate powder milled for 120 h: (a) bright-field image; insets show the presence of monocrystal ZrB_2 and TiB_2 ; (b) SAED pattern marked by an arrow

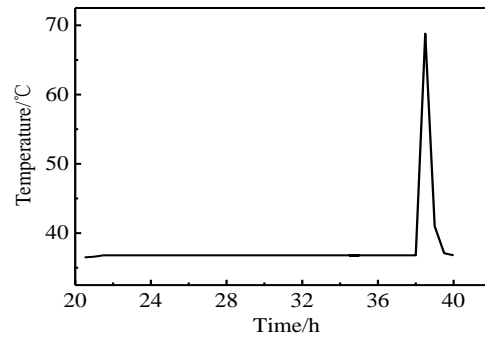


Fig.7 Temperature of the vial at the second stage

reaction is triggered in a localized area, it spreads quickly throughout in the mixture until the synthesis reaches completion. A sharp increase in the vial temperature indicates that the synthesis mechanism is a typical self-sustaining reaction induced by the ball milling (Fig.7).

In the third stage (>40 h), cold welding between the grains is limited due to the absence of a ductile component between the target products. With the increase of milling time, the particle sizes of the ZrB_2 and TiB_2 are continuously decreased (Fig.5).

3 Conclusions

1) A nanocrystalline ZrB_2 - TiB_2 powder can be synthesized by MA using a mixture of elemental Zr, Ti, and B powders at a Zr/Ti/B mole ratio of 1:1:4, a 10:1 ball-to-powder weight ratio, and a 500 rpm rotational speed in a planetary ball-mill under argon atmosphere using a ZrO_2 vial and balls.

2) The conversion of Zr, Ti, and B powders into ZrB_2 - TiB_2 is determined to be a self-sustaining reaction induced by the ball milling process.

3) The final product is comprised of nanoscale ZrB_2 (~20 nm) and TiB_2 (<20 nm) particles after 120 h of milling, with clear composites of the nanoscale TiB_2 particles and the ZrB_2 grains.

References

- Guo C, Chen J M, Yao R G et al. *Rare Metal Materials and Engineering*[J], 2013, 42 (8): 1547 (in Chinese)
- Qi G H, Fang C F, Bai Y et al. *Rare Metal Materials and Engineering*[J], 2011, 40(8): 1339 (in Chinese)
- Zhang J, Zhang D Q, Wu P W et al. *Rare Metal Materials and Engineering*[J], 2014, 43(1): 47 (in Chinese)
- Jiao L, Zhao Y T, Wu Y et al. *Rare Metal Materials and Engineering*[J], 2014, 43(1): 6 (in Chinese)
- Nasiri-Tabrizi B, Adhmi T, Ebrahimi-Kahrizsangi R. *Ceramics International*[J], 2014, 40(5): 7345
- Jalaly M, Bafghi M S, Tamizifar M et al. *Journal of Alloys and Compounds*[J], 2014, 588: 36

- 7 Xu L, Huang C, Liu H, Zou B et al. *International Journal of Refractory Metals and Hard Materials*[J], 2013, 37: 98
- 8 Wu W W, Zhang G J, Sakka Y. *Journal of Asian Ceramic Societies*[J], 2013, 1(3): 304
- 9 Qiu H Y, Guo W M, Zou J et al. *Powder Technology*[J], 2012, 217: 462
- 10 Ağaoğulları D, Gökçe H, Duman İ et al. *Journal of the European Ceramic Society*[J], 2012, 32(7): 1447
- 11 Avilés M A, Córdoba J M, Sayagués M J et al. *Ceramics International*[J], 2011, 37(6): 1895
- 12 Hu C, Sakka Y, Tanaka H et al. *Journal of Alloys and Compounds*[J], 2010, 494(1-2): 266
- 13 Peters J S, Cook B A, Haringa J L et al. *Wear*[J], 2009, 267(1-4): 136
- 14 Randich E. *Thin Solid Films*[J], 1979, 63(2): 309
- 15 Inagaki J I, Sakai Y, Uekawa N et al. *Materials Research Bulletin*[J], 2007, 42 (6): 1019
- 16 Klissurski D D R D. *Journal of Materials Synthesis and Processing*[J], 2001, 9(3): 131
- 17 Hwang P M T. *Journal of Materials Science*[J], 1996, 31(2): 351
- 18 Yin J, Huang Z, Liu X et al. *Materials Science and Engineering A*[J], 2013, 565: 414
- 19 Park Y H, Hashimoto H, Abe T. *Materials Science and Engineering A*[J], 1994, 181-182: 1291
- 20 Burmeister C F, Kwade A. *Chemical Society Reviews*[J], 2013, 42(18): 7660
- 21 Suryanarayana C. *Progress in Materials Science*[J], 2001, 46(1-2): 1
- 22 Li J, Li F, Hu K et al. *Journal of the European Ceramic Society*[J], 2001, 21(16): 2829
- 23 Yuan Q, Zheng Y, Yu H. *International Journal of Refractory Metals and Hard Materials*[J], 2009, 27(1): 121
- 24 Suryanarayana C, Al-Aqeeli N. *Progress in Materials Science*[J], 2013, 58(4): 383
- 25 Li Z, Wang W, Wang J I. *Advanced Powder Technology*[J], 2014, 25(1): 415
- 26 Chamberlain A L, Fahrenholtz W G, Hilmas G E. *Journal of the European Ceramic Society*[J], 2009, 29(16): 3401
- 27 Vallauri D, Atías Adrián I C, Chrysanthou A. *Journal of the European Ceramic Society*[J], 2008, 28(8): 169

机械合金化制备纳米 ZrB_2 - TiB_2 复合粉末

罗平^{1,2}, 董仕节^{1,2}, 杨李安卓², 孙世烜³, 谢志雄², 郑重², 杨巍²

(1. 华中科技大学, 湖北 武汉 430074)

(2. 湖北工业大学 湖北省绿色轻工材料重点实验室, 湖北 武汉 430068)

(3. 首都航天机械公司, 北京 100076)

摘要: 采用Zr、Ti、B为原料(摩尔比: 1:1:4), 在氩气气氛保护下, 采用机械合金化方式, 在球料比10:1、球磨转速500r/min 实验条件下制备了纳米结构的 ZrB_2 - TiB_2 。采用X射线衍射仪(XRD)、场发射扫描电镜(FESEM), 透射电镜(TEM)仪器, 对不同球磨时间粉末的相组成、微观结构进行了表征。结果发现, 原始粉末经120 h 球磨后, 粉末主要由 ZrB_2 和 TiB_2 组成, 平均尺寸在20 nm左右, TiB_2 分布于 ZrB_2 基体上。文章还探讨了该体系获得目标产物的机械合金化机制。

关键词: 二硼化锆-二硼化钛; 纳米复合材料; 机械合金化

作者简介: 罗平, 男, 1979年生, 博士生, 华中科技大学材料科学与工程学院, 湖北 武汉 430074, 电话: 027-5975077, E-mail: blueknight_0930@163.com